

---

---

# Vibration Monitoring for Defect Diagnosis on a Machine Tool: A Comprehensive Case Study

Mouleeswaran Senthilkumar, Moorthy Vikram and Bhaskaran Pradeep

Department of Production Engineering, PSG College of Technology, Coimbatore 641 004, India

(Received 31 July 2012; revised 17 December 2013; accepted 26 February 2014)

Vibration monitoring and analysis of machine tools are carried out in industry to reduce maintenance cost and downtime. In this case study, the application of vibration monitoring and analysis was carried out on a lathe. The characteristic frequencies of tapered roller bearings, gear mesh frequencies, and belt drive frequencies were found to locate the source of vibration. Multi-harmonics of fundamental defect frequencies were observed. From the real-time observation, experimental prediction of defects has been found to be correct and accurate. This case study shows that vibration analysis plays a vital role in monitoring the condition of the machine tool.

---

## NOMENCLATURE

$N_b$	Number of rollers
$n$	Revolutions per minute
$D$	Outer diameter, mm
$d$	Inner diameter, mm
$T$	Width, mm
$C$	Dynamic load rating, kN
$C_o$	Static load rating, kN
$P_u$	Fatigue load limit, kN
$m$	Mass, kg
$Z$	Number of gear teeth
$N$	Gear speed, rpm
$F_{gm}$	Gear meshing frequency, Hz
$F_b$	Belt drive frequency, Hz
$d_p$	Pulley diameter, mm
$N_p$	Pulley speed, rpm
$l_b$	Belt length, mm

## 1. INTRODUCTION

Vibration analysis is a measurement tool used to identify, predict, and prevent failures in machine tools. It involves the trending and analysis of machinery performance parameters to detect and identify problems before failure and extensive damage can occur. If problems can be detected early when the defects are minor and do not affect performance, and the nature of the problem can be identified while the machine runs, then repair time can be kept to a minimum, resulting in reduced machinery downtime. Therefore, vibration analysis is a technique that is employed to track machine operating conditions and trend deteriorations so as to reduce maintenance costs as well as downtime.<sup>1</sup> The vibration analysis technique consists mainly of vibration measurement and its interpretation. The vibration measurement is done by picking up signals from machines by means of vibration measurements. The signals are then processed using an FFT analyser to obtain the frequency spectrum. The results are mainly interpreted by relating the measured frequencies with their relevant causes such as unbalance, misalignment, bearing defects and resonance, etc. A case

study on vibration-based maintenance in paper mills has been presented to improve accuracy and effectiveness.<sup>2</sup>

There are many case studies on vibration monitoring and analysis of rotating machineries. Vibrations associated with rolling element bearings, especially ball bearings have been discussed extensively,<sup>3</sup> while applied statistical moments to bearings defect detection.<sup>4</sup> Two case studies present on the defect diagnosis of rolling element bearings.<sup>5,6</sup> Another case study has analysed the vibration of a centrifugal pump and investigated the spike energy of bearings in order to find out the source of the vibration.<sup>7</sup> In vibration analysis, an artificial neural network has also been employed to monitor and diagnose rolling element bearings.<sup>8</sup> In vibration diagnosis, it is found that not only rolling elements but other sources of vibration exist as well. Vibration analysis of a motor-flexible coupling-rotor system subjected to misalignment and unbalance has been studied extensively.<sup>9,10</sup> Characteristics of the torsional vibrations of an unbalanced shaft were also analysed in another study.<sup>11</sup>

This case study analyses the vibration produced in a lathe during the real operation at different machining conditions. The study has been made to identify defects in three major sources of vibration, namely, rolling element bearings, gears, and belt drives.

## 2. EXPERIMENTAL SETUP AND VIBRATION MEASUREMENT

Experiments on PSG 141 lathes have been conducted using the accelerometer, and these experiments have discovered the vibrations that formed. The technical details of the lathe and the experimental conditions are as follows:

Machine tool :	PSG 141 lathe
Machine speed (rpm) :	38 60 71 90 115 140 200 250 228 360 450 580 740 800 1150 1600
Power :	Std. motor for main drive 1.1/2.2 kW (For 16 speeds) 1440/2880 rpm, 415 V, 3 phase, 50 Hz, AC

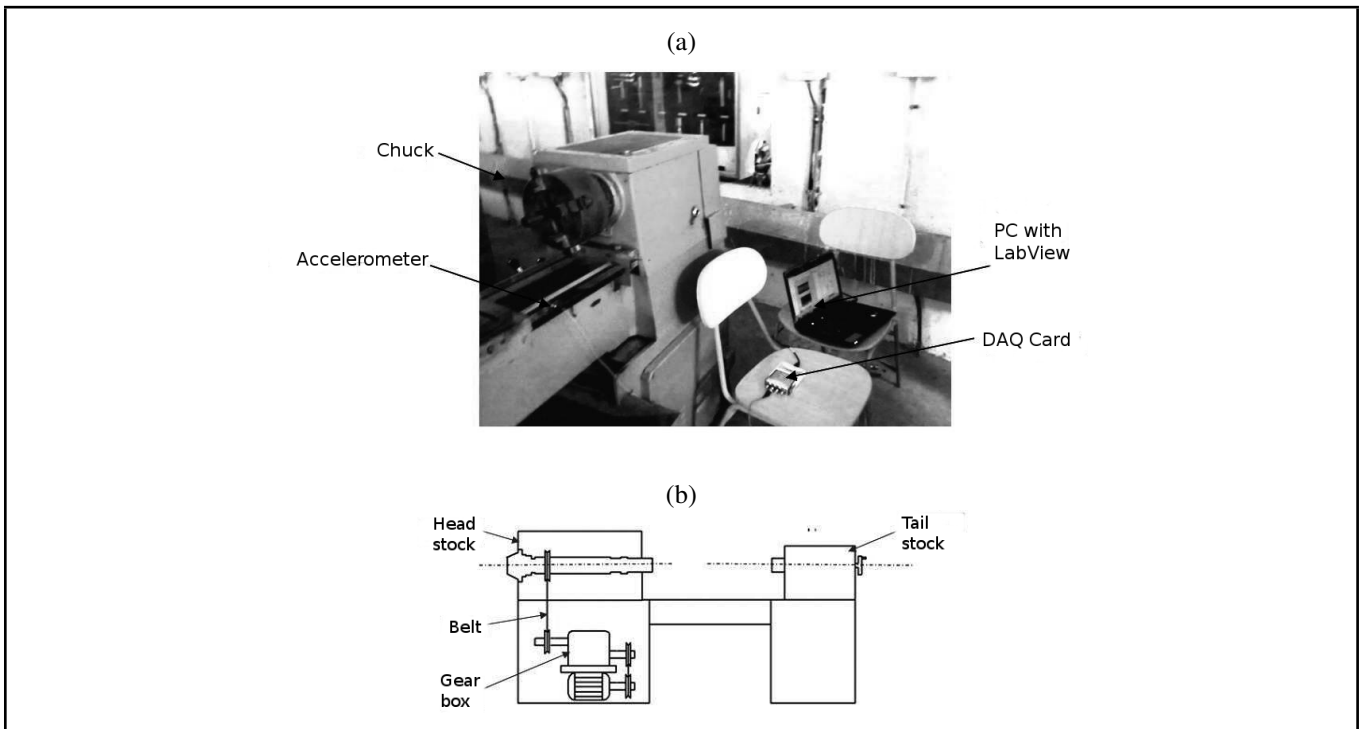


**Figure 1.** a) Experimental setup (Machine tool with data acquisition system); b) Schematic layout of drive system of the machine tool.

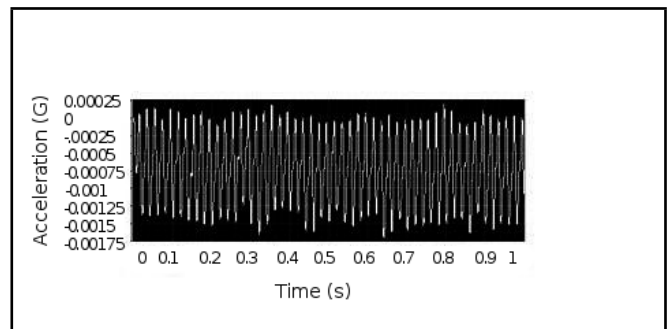
Height of centre : 177.5 mm  
 Admit between centres : 800 mm  
 Operation : Turning  
 Component : Cylindrical component of Fig- diameter 25 mm and length 70 mm  
 Depth of cut : 0.5 mm

Figure 1 shows the experimental setup along with the position of the accelerometer. We collected the vibration data using the general purpose DYTRAN 3097A2 accelerometer with a sensitivity of  $100 \frac{mV}{g}$  in a frequency range of 0.3 Hz–10 kHz. Vibration measured in the vertical directions was dominant compared with the other two directions; hence they are only used to characterize the health of the machine tool. The accelerometer signals were taken to PC via the NI 9234 data acquisition card system using LabVIEW software.

The vibration of the machine tool is measured in three different locations: the lathe bed (simply supported), the head stock (bearing mountings), and the compound rest (tool and work piece interaction). These locations are vibration prone areas and result in higher vibration than other locations. The measurement is first taken in the lathe bed for different speeds. The peak frequencies appeared in the amplitude-versus-frequency spectrum, and all the speeds measured are the same and are found to be 50 Hz, 100 Hz, 150 Hz, 200 Hz, 350 Hz, 400 Hz and 450 Hz. The time-domain and frequency-domain data at 90 rpm and 800 rpm are shown in Figs. 2-5.

The frequency spectrums shown in Figs. 6-7 were taken on the head stock of the lathe. The peak frequencies obtained for four different spindle speeds (90, 200, 450 and 800 rpm) are found to be 70 Hz and 220 Hz, whereas the peak frequencies obtained for 1600 rpm are 160 Hz, 220 Hz, and 270 Hz.

Similarly, the vibration data for the compound rest was taken and is shown in Figs. 8-9. The peak frequencies that appeared



**Figure 2.** Time domain data of the lathe bed at 90 rpm.

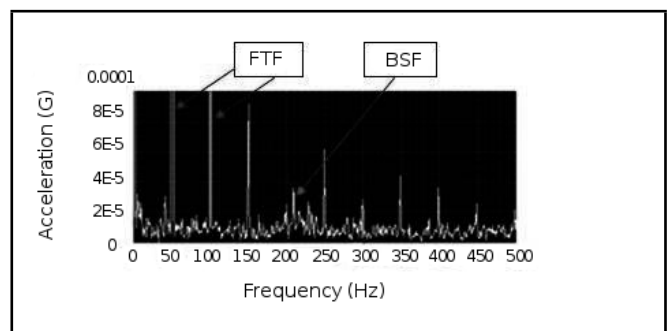


**Figure 3.** Frequency spectrum of the lathe bed at 90 rpm.

for all the spindle speeds (90 rpm, 200 rpm, 450 rpm, 800 rpm, and 1600 rpm) are the same and are found to be 50 rpm, 100 rpm, 150 rpm, 250 rpm, 350 rpm, and 400 Hz.

### 3. RESULTS AND DISCUSSION

Forces generated within the machine cause vibration. Sources of vibration in a typical machine tool like a lathe includes misalignment of couplings, bearings, unbalance of rotating components, looseness, deterioration of rolling element

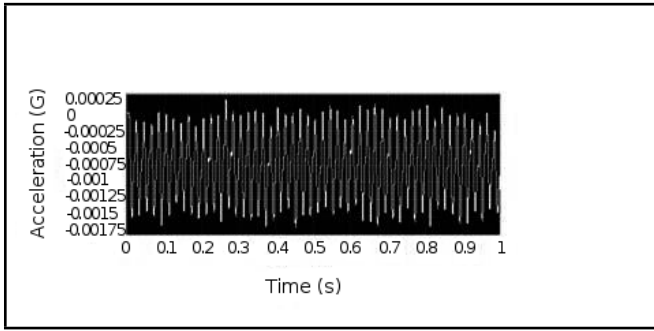


Figure 4. Time domain data of the lathe bed at 800 rpm.

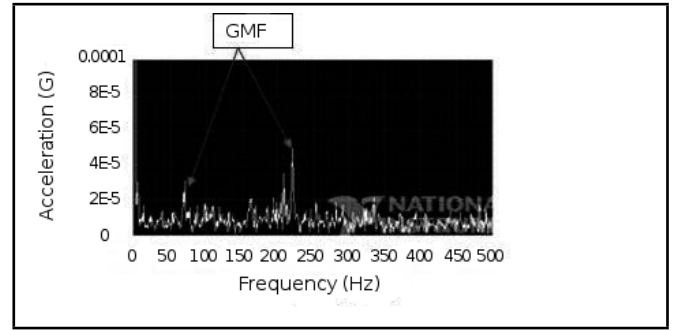


Figure 7. Multi-harmonics of the bearing defect frequencies at 450 rpm.

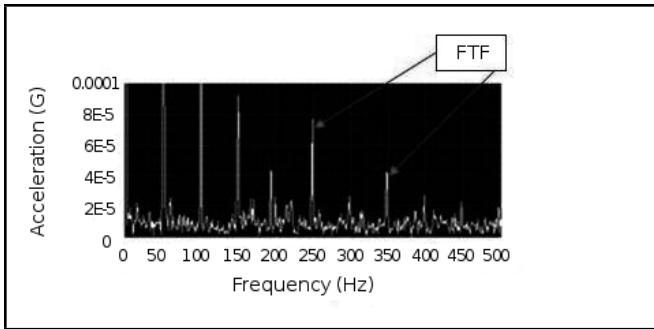


Figure 5. Frequency spectrum of the lathe bed at 800 rpm.

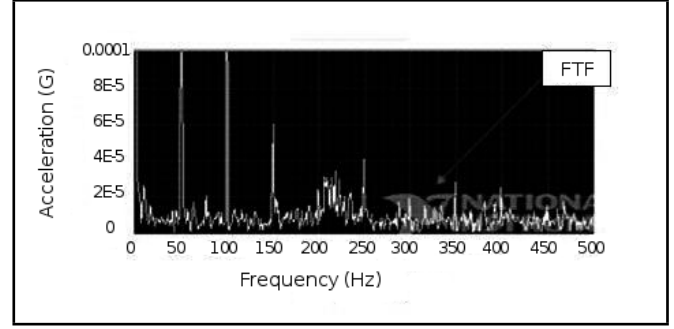


Figure 8. Frequency spectrum of the compound rest at 90 rpm.

bearings, gear wear, resonance, and the eccentricity of rotating components such as V-pulleys or gears, etc. Therefore, it is important to calculate the characteristic frequencies of the three major sources of vibration in a machine tool, namely, the tapered roller bearing, the gear mesh, and the belt drive. The calculated characteristic frequencies are attempted to be matched with experimental peak frequencies. The faults in these elements caused peaks to develop at their characteristic frequencies, which indicate their possible presence. Referring to Fig. 1b, the belt drive connecting the motor and gear box provides a gear reduction ratio of 2.58. The drive connecting the gear box and the head stock results in a gear reduction ratio of 1.14.

### 3.1. Tapered Roller Bearing Defect Frequencies

Two tapered roller bearings are each installed at the front and rear ends of the lathe spindle. The front end of the spindle is fitted with the 32212 J2/Q bearing, and the rear end is fitted with the 32209 J2/Q bearing. Figure 10 shows the rolling el-

ement bearing geometry. The main geometric dimensions are listed in Table 1. In a previous study, rolling element bearing defect frequencies are found out by using the Eqs. (1)-(4):<sup>7</sup>

Ball pass frequency of inner race way (BPFI):

$$BPFI = \left( \frac{N_b}{2} + 1.2 \right) n, \text{ Hz.} \quad (1)$$

Ball pass frequency of outer race way (BPFO):

$$BPFO = \left( \frac{N_b}{2} - 1.2 \right) n, \text{ Hz.} \quad (2)$$

Ball spin frequency (BSF):

$$BSF = \frac{1}{2} \left( \frac{N_b}{2} - \frac{1.2}{N_b} \right) n, \text{ Hz.} \quad (3)$$

Fundamental train frequency of the cage or retainer (FTF):

$$FTF = \left( \frac{1}{2} - \frac{1.2}{N_b} \right) n, \text{ Hz.} \quad (4)$$

The basic assumptions made are: all rollers are of equal diameter, pure rolling contact exists between rollers and the outer

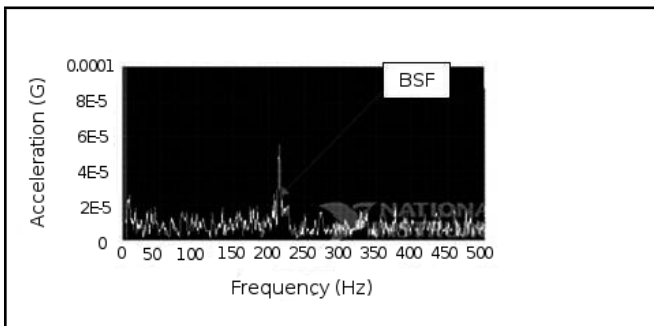


Figure 6. Frequency spectrum of the headstock at 90 rpm.

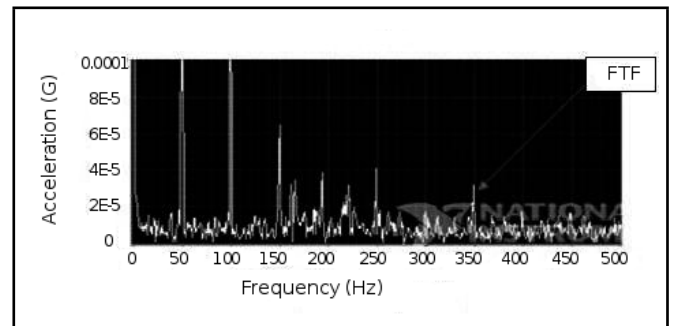


Figure 9. Frequency spectrum of the compound rest at 800 rpm.

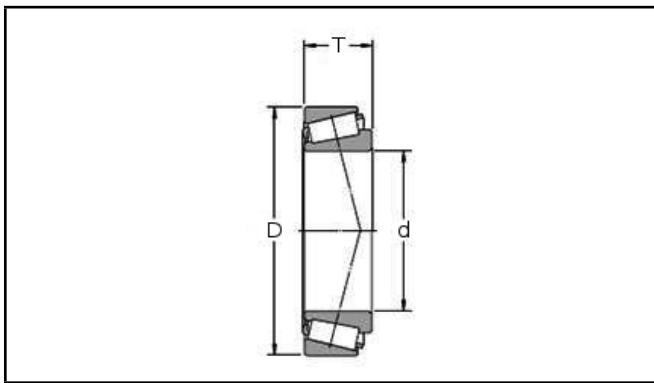


Figure 10. Rolling element bearing geometry.

Table 1. Geometric dimensions of the bearings of the head stock spindle.

Parameters	Front end 32212 J2/Q	Rear end 32209 J2/Q
<i>D</i>	110	85
<i>d</i>	60	45
<i>T</i>	29.75	24.75
<i>N<sub>b</sub></i>	19	19
<i>C</i>	146	91.5
<i>C<sub>o</sub></i>	160	98
<i>P<sub>u</sub></i>	18.6	11
<i>m</i>	1.15	0.58

race, no slipping occurs between the shaft and the bearing, and the outer race is stationary. Both these bearings have a contact angle of 0°. Also, as there is a very small thrust; it is neglected.

The spectrums were captured, and the certain defect related frequencies of the bearings have been identified and encircled in Table 2. Hence we tried to identify any such peaks there are in the spectrum. The harmonics (sub & super) of different spindle speeds are found out and tabulated in Table 2. It is found that the calculated fundamental bearing defect frequencies for the different speeds are found to be deviated from the experimentally measured peak frequencies. However, the superharmonics (1.5X and 2.5X) of the fundamental train frequency of the retainer were found to match with the peak frequencies at lower speeds. Subharmonics of the same were also found to match with the peak frequencies at higher speeds. Also, Figs. 3, 5, 8, and 9 indicate that the retainer is defective; hence, we anticipated that the retainer or cage would be defective.<sup>7</sup> So, the bearings were dismantled and examined. We identified the front end bearing as having defective retainers.

### 3.2. Gear Mesh Frequencies in Gear Box and Headstock

Apart from bearing characteristic frequencies, there are many other peak frequencies found from the spectrums. Therefore, it was necessary to track other defective elements like gears in the gear box and head stock. Fig. 11a shows the gear train arrangement in the lathe under study, whereas Fig. 11b depicts the inner view of the gear box. The identification of possible gear problems is fairly easy since the most common vibration frequencies will be equal to the harmonics of the gear meshing frequency. The gear meshing frequency ( $F_{gm}$ ) is referred to as:<sup>12</sup>

$$F_{gm} = \frac{ZN}{60}, \text{ Hz.} \tag{5}$$

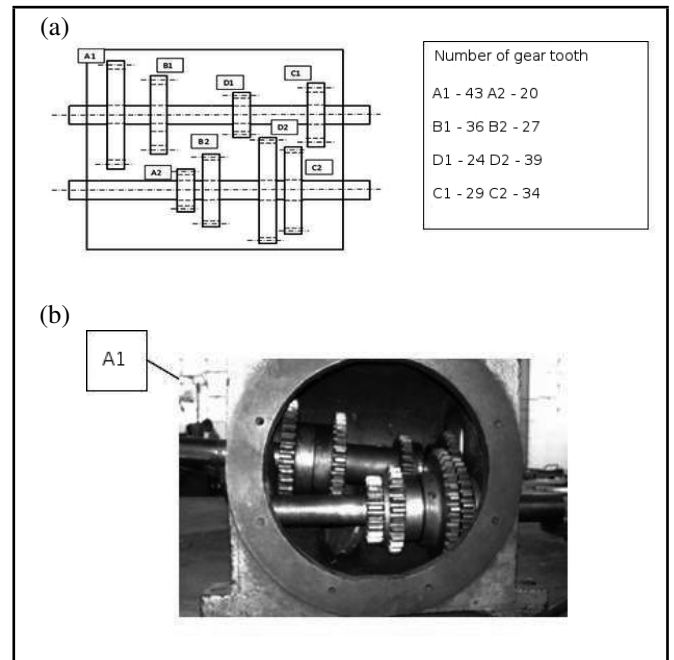


Figure 11. a) Gear train layout of main gear box; b) Inner view of main gear box.

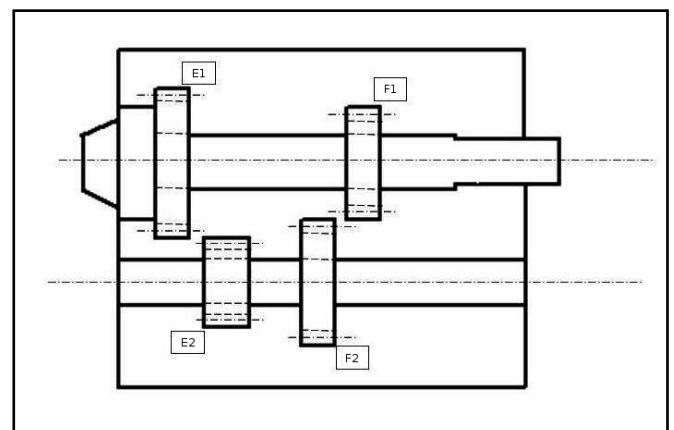


Figure 12. Gear box layout in head stock.

The experimental data at different spindle speeds are tabulated in Table 3. Inspection of Table 3 shows that 150 Hz is equivalent to the 0.5X at 90 rpm and 0.25X at 200 rpm. At different speeds, the subharmonics of the gear meshing frequency also match with the peak frequencies. This indicates that the gears in the gear box are defective. Further evidence is required to identify the exact defective gear pairs. Table 4 depicts how the power and speed flow from the drive motor to the spindle. Different spindle speeds have been achieved by engaging different sets of gears in the gear box and the head stock as shown in Table 4. This will be helpful in identifying the faulty gear pairs that develop peak frequencies. Figure 12 shows the gear train arrangement in the head stock. Table 5 shows the harmonics of the gear meshing frequency of the head stock.

From the Table 5, we observed that the subharmonics of the gear mesh frequencies match with the peak frequencies at almost all speeds. It clearly depicts that the gears are defective in the head stock as well.

**Table 2.** Multi-Harmonics of bearing defect frequencies.

Defect	Subharmonics			Fundamental frequency (Hz)	Superharmonics		
	0.25X	0.5X	0.75X		1X	1.5X	2X
Spindle speed: 90 rpm							
BPFI	240.75	481.5	722.25	963	1444.5	1926	2407.5
BPFO	186.75	373.5	560.25	747	1120.5	1494	1867.5
BSF	106.16	212.32	318.48	424.65	636.97	849	1061.62
FTF	9.82	19.65	29.48	39.31	<b>58.96</b>	78.62	<b>98.27</b>
Spindle speed: 200 rpm							
BPFI	535	1070	1605	2140	3210	4280	5350
BPFO	415	830	1245	1660	2490	3320	4150
BSF	235.82	471.84	707.6	943.68	1415.52	1887	2359.2
FTF	21.84	<b>43.68</b>	65.52	87.36	131.04	174	218.4
Spindle speed: 450 rpm							
BPFI	1203.75	2407.5	3611.25	4815	7222.5	9630	12037.5
BPFO	933.75	1867	2801	3735	5602	7470	9338
BSF	530	1061	1592	2123.28	3184	4246	5308
FTF	<b>49.14</b>	<b>98.25</b>	<b>147.42</b>	196.56	294.84	<b>393.12</b>	491.4
Spindle speed: 800 rpm							
BPFI	2140	4280	6420	8560	12840	17120	21400
BPFO	1660	3320	4980	6640	9960	13280	16600
BSF	943.68	1887.3	2831	3774.7	5662	7549	9436
FTF	87.36	174.7	262	<b>349.44</b>	524.16	698.8	873.6
Spindle speed: 1600 rpm							
BPFI	4280	8560	12840	17120	25680	34240	42800
BPFO	3320	6640	9960	13280	19920	26560	33200
BSF	1887	3774	5662	7547	11324	15098	18873
FTF	174.7	<b>349.44</b>	524.16	698.08	1048.32	1397	1747

**Table 3.** Multi-harmonics of gear mesh frequencies in the gear box.

Spindle speeds(rpm)	Subharmonics				Superharmonics		
	0.25X	0.5X	0.75X	1X	1.5X	2X	2.5X
90	79	<b>158</b>	237.10	316.14	474.2	632.2	790.3
200	<b>158</b>	316.14	474.2	632.2	948.3	1264.5	1580.7
450	<b>92.98</b>	185.9	278.9	371.9	557.9	743.8	929.8
800	90.66	181.3	<b>271.9</b>	362.6	543.9	725.28	906
1600	181.32	362.6	543.9	725.29	1087	1450	1813

**Table 6.** Multi-harmonics of belt drive frequencies.

Spindle speeds (rpm)	Subharmonics				Superharmonics		
	0.25X	0.5X	0.75X	1X	1.5X	2X	2.5X
90	36.6	73.3	110	<b>146.6</b>	220	293.3	366
200	73.4	<b>146.8</b>	<b>220.2</b>	293.6	440.5	527	659
450	29.1	<b>58.2</b>	87.3	116.5	174.7	233	291
800	<b>50.8</b>	<b>101.7</b>	152.6	203.5	305.2	407	508
1600	<b>101</b>	203	305	407	610	814	1017

### 3.3. Belt drive frequencies

In order check whether or not the belt drive is the source of some vibrations, the belt drive system was also analysed. Vibration due to belt problems implies that there is something physically wrong with the belts themselves such as hard spots, missing chunks, or other belt deformities that produce dynamic forces with characteristic vibration frequencies, which are directly related to the rotating speed (rpm) of the belts.<sup>13</sup> Belt drive frequency is determined from:

$$F_b = \frac{\pi d N_p}{l_b}, \text{ Hz.} \tag{6}$$

From the harmonics of the belt drive frequencies as given in Table 6, it was observed that 0.5X and 0.75X of 200 rpm

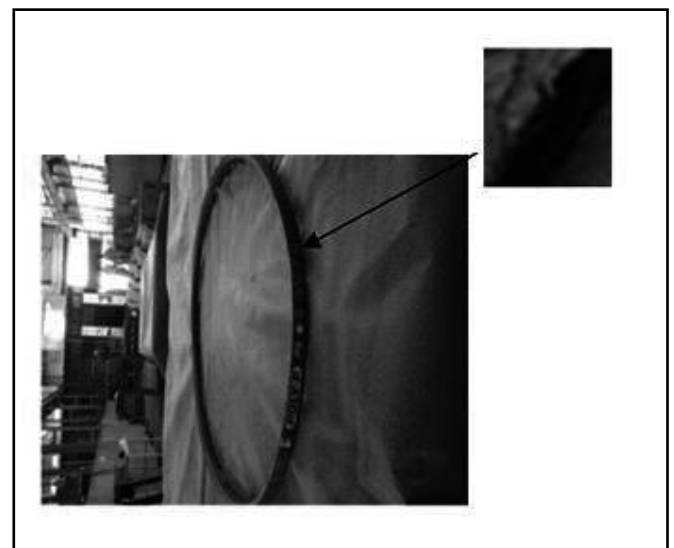


**Figure 13.** Defective belt in the drive system.

appeared at 150 Hz and 220 Hz, 0.25X and 0.5X at 800 rpm both appeared at 50 Hz, and 0.25X of 1600 rpm appeared at 100 Hz. Hence a defect in the belt has been found out, and the defective belt is shown in Fig 13.

**Table 4.** Drive (gear pair) engagement for different spindle speeds.

Input Motor speed (rpm)	Engagement of 1 <sup>st</sup> Belt drive	Gears Engaged in Gear Box	Engagement of 2 <sup>nd</sup> Belt drive	Gears Engaged in Head Stock	Spindle Speed (rpm)
1440	✓	C1-C2	✓	E1-E2	90
2880	✓	C1-C2	✓	E1-E2	200
2880	✓	A1-A2	✓	F1-F2	450
1440	✓	D1-D2	✓	F1-F2	800
2880	✓	D1-D2	✓	F1-F2	1600

**Table 5.** Multi-harmonics of gear mesh frequencies.

Spindle speeds(rpm)	Subharmonics				Superharmonics		
	0.25X	0.5X	0.75X	1X	1.5X	2X	2.5X
90	38.28	<b>76.56</b>	114.84	<b>153.13</b>	229.69	306.26	382.82
200	<b>76.56</b>	<b>153.13</b>	229.7	306.27	459.4	612.54	765.675
450	<b>113.91</b>	227.82	<b>341.73</b>	455.64	683.46	911.28	1139.1
800	198.98	<b>397.9</b>	596.96	795.95	1193.92	1591.9	1989.8
1600	<b>397.97</b>	795.95	1193.92	1591.9	2387.8	3183.8	3979.75

## 4. CONCLUSION

In this study, the defect diagnosis of a machine tool (lathe) using the spectrum analysis technique is carried out. The bearing defect frequencies were evaluated and compared with the measured data, which indicates defects in the cage of the tapered roller bearing. Harmonics of gear mesh frequencies were calculated, and it was discovered that defective gear pairs in the gear box and the head stock existed. By calculating the belt drive frequency and its harmonics, defects in the belt drive were also confirmed. Hence, a recommendation of dismantling the lathe drive system and the replacement of the bearing, the defective gear pairs, and the belt drive was sent to the maintenance group.

## REFERENCES

- Renwick, J. T. and Babson, P. E. Vibration analysis-a proven technique as a predictive maintenance tool, *IEEE Tran. Ind. Appl.*, **21**(2), 324–32, (1985).
- Al-Najjar, B. Accuracy, effectiveness and improvement of vibration-based maintenance in paper mills: case studies, *J. Sound Vib.*, **229**(2), 389–410, (2000).
- Gohar, R. and Aktuřk, N. Vibrations associated with ball bearings, *ImechE*, 43–64, (1998).
- Martin, H. R. and Honarvar, F. Application of statistical moments to bearing failure detection, *Applied Acoustics*, **44**, 67–77, (1995).
- Heng, R. B. W. and Nor, M. J. M. Statistical analysis of sound and vibration signals for monitoring rolling element bearing condition, *Applied Acoustics*, **53**(1-3), 221–226, (1998).
- Orhan, S., Akturk, N., and Celik, V. Vibration monitoring for defect diagnosis of roller element bearings as a predictive maintenance tool: comprehensive case studies, *NDT&E International* **39**, 293–298, (2006).
- Fathi, N and Mayo, F. Beating phenomenon of multi harmonics defect frequencies in rolling element bearing: case study from water pumping station, *World Academy of Science, Engineering and Technology*, **57**, (2009).
- Alguindigue, I. E., Buczak, L. A., and Uhrig, R.E. Monitoring and diagnosis of rolling element bearings using artificial neural networks, *IEEE Trans Ind Electron*, **40**(2), 209–17, (1993).
- Xu, M. and Marangoni, R. D. Vibration analysis of a motor-flexible coupling-rotor system subject to misalignment and unbalance, part II: experimental validation. *J. Sound Vib.*, **176**(5), 681–694, (1994).
- Senthil kumar, M. and Sendhil kumar, S. Effects of misalignment and unbalance in a vibration analysis of rotor-bearing systems, *National Journal of Technology*, **8**(1), (2012).
- Huang, D. G., Characteristics of torsional vibrations of a shaft with unbalance, *J. Sound Vib.*, **308**, 692–698, (2007).
- Dalpiaz G., Rivola A. and Rubini Dynamic modelling of gear systems for condition monitoring and diagnostics, *Proc. Congress on Technical Diagnostics*, Bologna, Italy, (1996).
- Cornelius, S. and Paresh, G. Practical Machinery Vibration Analysis and Predictive Maintenance, *Elsevier*, (2004).